Process Safety and Environmental Protection 158 (2022) 547–559

Contents lists available at ScienceDirect

Process Safety and Environmental Protection

journal homepage: www.elsevier.com/locate/psep

# Anaerobic co-digestion of tannery effluents: Process optimisation for resource recovery, recycling and reuse in a circular bioeconomy

A.B. Mpofu[a,b], W.M. Kaira[a,b], O.O. Oyekola[a], P.J. Welz[b,*]

[a] Department of Chemical Engineering, Cape Peninsula University of Technology, Bellville Campus, Symphony Way, Cape Town 7535, South Africa
[b] Institute of Applied Microbial and Health Biotechnology Institute, Cape Peninsula University of Technology, Bellville Campus, Symphony Way, Cape Town 7535, South Africa

ARTICLE INFO

*Article history:*
Received 20 September 2021
Received in revised form 1 December 2021
Accepted 11 December 2021
Available online 16 December 2021

*Keywords:*
Tannery effluents
Anaerobic co-digestion
Kinetics
Optimisation
Resource recovery
Circular bioeconomy

ABSTRACT

The anaerobic treatment of tannery effluents from the different process stages are limited by the various toxicants that are mainly added as feed chemicals. The segregated effluents present an opportunity for co-treatment to abate inhibition, supplement deficient nutrients and/or promote resource recovery using anaerobic digestion. This study investigated the feasibility of anaerobic co-digestion of beamhouse (BH) and pre-treated tanyard (TY) effluents using the standardised biochemical methane potential (BMP) protocol. It was established that all reactors were active, while those with higher TY compositions and operating at very high/low inoculum to substrate ratios ($3 < ISR \leq 2$) suffered severe methanogenesis inhibition. Process efficiency and kinetics (maximum $CH_4$ production rate and reaction rate constant) improved with increasing BH composition and/or ISR. The logistic, modified Gompertz and cone model showed a better fit to the experimental cumulative $CH_4$ data ($0.827 \leq Adj\ R^2 \leq 0.999$), respectively. The optimal operating conditions (ISR = 2.5, 100% BH and 20 days retention time) demonstrated the feasibility of a circular bioeconomy and net positive tannery operations where 639 mL biogas/gVS (59% $CH_4$), 13% and 18% of the inlet sulphur and nitrogen, respectively, are recoverable as products. The process also recovered reusable process/irrigation water, recyclable digestate as a biofertiliser and/or ceramic aggregate with energy recovery.


## 1. Introduction

The leather industry is a strategically important sector for the socioeconomic development of third world countries that dominate the industry. Leather products are amongst the most commonly traded commodities globally (Buljan and Král, 2015). The industry prevents the disposal of skins/hides from the meat and dairy industry by recycling them into leather. However, the industry is generally regarded as a heavy polluter due to its linear economy that dictates the disposal of about 20–40 $m^3$ of complex effluents, 450–730 kg of solid waste, and 500 kg of wet wastewater sludge laden with residual processing chemicals per tonne of tanned raw skins/hides (Buljan and Král, 2015, 2019). The process wastes about 380 kg (84%) of the feed chemicals per tonne of processed skins/hides (Buljan and Král, 2019). The final quantitative and qualitative characteristics of tannery effluents depend on the tannery and wastewater treatment operations (Table 6, Supplementary).

Physicochemical treatments, coupled with the conventional activated sludge process are mostly used to remediate tannery effluents (TE). Tanneries generally separate effluent streams into soaking, beamhouse (BH), tanyard (TY) and general effluent in order to maintain simplicity in the tannery wastewater treatment plant (WWTP). The BH operations contribute more than 80% of the organic pollution load and about 40–70% of ammonia nitrogen ($NH_3$-N)) in TE while TY processes contribute more than 90% chrome (Cr) and 60% sulphate ($SO_4^{2-}$) (Buljan and Král, 2019). The chromium contained in TY effluents is mainly Cr (III) and/or Cr (VI) which is more toxic, carcinogenic, and mutagenic even in trace quantities. High sulphide levels contained in BH effluents may be released as a gas if mixed with acidic effluents such as TY effluent. Other microbial toxicants such as ammonia ($NH_3$), toxic metals, sulphate ($SO_4^{2-}$), sulphide ($H_2S$) and volatile organic acids (VOA) may be diluted and/or exacerbated by mixing streams. Nonetheless, tanneries still struggle to effectively treat separated streams to comply with the stipulated discharge standards, and to deal with enormous excess sludge. There are a number of studies that have reported on environmental pollution by tanneries in the developing world, where

* Corresponding author.
*E-mail address:* welzp@cput.ac.za (P.J. Welz).

https://doi.org/10.1016/j.psep.2021.12.027
0957-5820/

the quest for economic development seems to have outweighed the need for environmental protection to varying extents.

In line with the current circular economy principles and sustainable development, tanneries are capable of preventing waste generation and environmental pollution by promoting resource conservation, recovery, recycling and reuse. However, the adoption of cleaner production techniques in developing countries is traditionally slow as tanners are reluctant to adapt their tanning processes due to their perception that these may jeopardise the quality of the leather produced (Buljan and Král, 2019). Additionally, sophisticated equipment and specialty chemicals are generally expensive and require higher capital investments. A review by Mpofu et al. (2021a) reported on the potential of converting tannery WWTPs into biorefineries through implementation of AD for the recovery of reusable, and recyclable value-added products such as bioenergy (methane, hydrogen or biomass), organic acids, sulphur, metals, construction aggregate, biofertiliser/compost, and/or 'fit for purpose' water reuse. However, the application of AD is affected by nutrient imbalance, deficiency and/or inhibition and this can be potentially abated through co-digestion (AcoD) of segregated TEs. This eliminates additional costs for the transportation of co-substrates from other industries.

Previous studies by Agustini et al. (2019); Berhe and Leta (2018); Mekonnen et al. (2016) and Vazifehkhoran et al. (2018) successfully codigested general (combined) TEs with tannery solid wastes (leather shavings, sludge and/or fleshings), cow dung, and fresh wheat straw (*Triticum aestivum*), respectively, for biogas (methane) recovery. Achouri et al. (2017) investigated the AcoD of BH and a combined TY and dyehouse effluent at 50% volumetric composition after their pretreatment with ferric chloride (coagulation). Majority of the previous studies including mono digestion did not explicitly describe the type or source of the TE used, and only provided a limited number of effluent physicochemical parameters (Mpofu et al., 2021a). To the authors' knowledge there are no studies investigating the AcoD of bovine/ovine BH and TY effluents at varying volumetric (%v/v) and inoculum to substrate (ISR) ratios for resource recovery other than biogas (methane) and/or the determination of process kinetics. Therefore, the purpose of this study was to optimise the AcoD of BH and TY effluents for the recovery of recyclable/reusable resources at varying volumetric substrate to substrate ratios [SSR (v/v)], and inoculum to substrate ratios (ISR). The study also sought to bridge the research gap by (i) comprehensively characterising the BH and TY effluents from a bovine/ovine tannery (ii) modelling and determining the kinetics of the AcoD process and (iii) demonstrating the feasibility of a circular bioeconomy that promotes net positive tannery operations with potential cost savings.

## 2. Materials and methods

### 2.1. Sampling

Tannery effluent samples were collected from a local tannery in South Africa that processes about 3500–4000 bovine hides and 5000–8000 ovine skins per day via wet-blue tanning. Grab samples of BH and pre-treated TY streams were taken to form six monthly composites of about 50 L over the course of 6 months to allow for fluctuations in effluent quality.

### 2.2. Analytical methods

A Merck Spectroquant Pharo® Spectrophotometer (Darmstadt, Germany) together with Merck cell tests/kits, ion-chromatography, inductively coupled plasma (ICP) atomic emission spectroscopy (AES) and loss of mass on ignition standard methods were used to determine the physicochemical characteristics of TEs as described by Mpofu et al. (2020, 2021b). The methane ($CH_4$), carbon dioxide ($CO_2$), and oxygen ($O_2$) content (%vol), as well as the $H_2S$ content (parts per million (ppm)) of the biogas were determined using a Geotech biogas 5000 analyser (Warwickshire, England) according to the manufacturers' instructions. Biogas volume was determined using a luer lock gas tight syringe (Lasec, South Africa).

### 2.3. Biomethane potential experiments

The biomethane potential protocol (BMP) described by Holliger et al. (2016) was followed in this study. Thirteen bioreactors for AcoD experiments were set up following a full factorial central composite design (CCD) for ISR (1–4) and SSR (0–100% BH) as variables. Three duplicate sets of four bioreactors were set up for (i) duplicate axial points for AcoD experiments, (ii) mono anaerobic digestion experiments and (iii) negative control experiments. This experimental design was created using Design-Expert® Software Version 10 (Stat-Ease, Inc., Minneapolis, USA). Validation experiments were set up to validate the determined theoretical optimum conditions. A viable acclimated inoculum was prepared by feeding a 50/50 (v/v) of BH and TY to digestate obtained from a mesophilic batch reactor treating ostrich TE. A constant volume of inoculum was added in all reactors, while the volume of blended BH and TY varied depending on the desired SSR and ISR. Detailed information on the experimental set up and operation is described elsewhere by Mpofu et al. (2021b).

### 2.4. Kinetic study

The kinetics of the BMP reactors were evaluated by fitting the modified Gompertz, first order, Logistic, Cone, and Chen and Hashimoto (C&H) models onto the cumulative $CH_4$ yield data using non-linear regression method. These kinetic models were selected as they display a sigmoidal shape which adequately describes the lag, exponential and stationary phases expected during the AD of TE. Statistical measures that were used to test for models' goodness of fit were adjusted coefficient of determination (Adj $R^2$), F test, Akaike's Information Criterion (AIC), and the root mean square error (RMSE).

## 3. Results and discussion

### 3.1. Characterisation of tannery effluents

It is known that there is considerable intra and inter-site variation in TE characteristics due to differences in tannery operations and in wastewater treatment processes. The characteristics of BY and TY effluents were within the concentration ranges reported in literature (Mpofu et al., 2021a) and their variation over time are discussed below. This demonstrates the need to mention the type or source of the characterised TE as the concentrations vary.

#### 3.1.1. Chemical and biological oxygen demand and solids concentrations in the bovine/ovine tannery effluents

The characteristics of the bovine/ovine (BOTE) exhibited a batch-to-batch variation (Tables 1a and 1b). Variations in TS, TVS, BOD and COD of both BH and TY effluents were insignificant (ANOVA, $p > 0.05$). The TS, TVS, BOD and COD concentrations of BH were notably higher than those in the TY, but the BOD:COD ratios of the TY (0.36–0.61) were higher than those of the BH (0.18–0.32). The

**Table 1a**
Characteristics of beamhouse bovine/ovine tannery effluent.

| Parameter | Batch 1 | Batch 2 | Batch 3 | Batch 4 | Batch 5 | Batch 6 | Mean | SD ± |
|---|---|---|---|---|---|---|---|---|
| **TOC** (mg/L) | 9250 | 7240 | 5160 | 4710 | 4220 | 3540 | 5687 | 2150 |
| **COD** (mg/L) | 24650 | 20350 | 27725 | 21675 | 23180 | 26200 | 23963 | 2776 |
| **BOD** (mg/L) | 7500 | 6500 | 5000 | 6000 | 6000 | 7000 | 6333 | 876 |
| **$VOA_t$** (mg/L AAE) | 2637 | 3109 | 4173 | 2674 | 2007 | 2691 | 2882 | 724 |
| **TN** (mg/L) | 1035 | 1320 | 1020 | 1315 | 1600 | 1430 | 1287 | 226 |
| **TAN** (mg/L $NH_3$ – N) | 865 | 96 | 136 | 230 | 176 | 313 | 303 | 286 |
| **$NO_3$** (mg/L) | 5.90 | 4.70 | 3.15 | 5.85 | 5.15 | 4.10 | 4.81 | 1.06 |
| **$NO_2$** (mg/L) | 0.30 | 12.2 | 10.6 | 1.10 | 1.30 | 1.60 | 4.5 | 5.4 |
| **TP** (mg/L $PO_4^{2-}$ – P) | 63.2 | 4.95 | 5.9 | 7.5 | 10.6 | 40.9 | 22.2 | 24.3 |
| **$SO_4^{2-}$** (mg/L) | 1120 | 2400 | 2200 | 1130 | 1450 | 1850 | 1692 | 545 |
| **$HS^-$** (mg/L) | 0.40 | 476 | 276 | 456 | 1.88 | 0.60 | 202 | 231 |
| **Cl** (mg/L) | 2500 | 3175 | 9025 | 6825 | 8125 | 8840 | 6415 | 2885 |
| **TS** (g/L) | 31.4 | 30.5 | 38.0 | 46.5 | 34.0 | 32.7 | 35.5 | 6.01 |
| **TVS** (g/L) | 11.6 | 9.83 | 14.4 | 18.9 | 10.9 | 11.8 | 12.90 | 3.30 |
| **Proteins** (mg/L) | 1562 | 2610 | 2090 | 3931 | 4184 | 2871 | 2875 | 1024 |
| **K** (mg/L) | 45.6 | 78.5 | 99.6 | 129 | 126 | ND | 95.7 | 34.8 |
| **Na** (mg/L) | 5552 | 6446 | 6058 | 6820 | 7184 | ND | 6412 | 638 |
| **Fe** (mg/L) | 0.05 | 0.03 | 0.08 | 0.26 | 0.13 | ND | 0.111 | 0.09 |
| **Ca** (mg/L) | 497 | 254 | 199 | 1091 | 1419 | ND | 692 | 539 |
| **Mg** (mg/L) | 375 | 60.3 | 151 | 3.70 | 11.8 | ND | 120 | 154 |
| **Zn** (µg/L) | 169 | 432 | 158 | 739 | 996 | ND | 499 | 366 |
| **Cu** (µg/L) | 21.8 | 13.8 | 10.9 | 26.7 | 167.9 | ND | 48.2 | 67.2 |
| **Co** (µg/L) | 1.79 | 2.57 | 2.84 | 4.36 | 2.74 | ND | 2.86 | 0.93 |
| **Cd** (µg/L) | 0.00 | 0.00 | 0.00 | 0.09 | 0.32 | ND | 0.083 | 0.14 |
| **Ni** (µg/L) | 26.48 | 30.9 | 28.9 | 21.9 | 25.9 | ND | 26.8 | 3.40 |
| **Cr** (µg/L) | 136 | 62.6 | 155 | 66.0 | 38.8 | ND | 91.8 | 50.8 |
| **Pb** (µg/L) | 2.90 | 2.31 | 2.15 | 4.57 | 8.25 | ND | 4.04 | 2.55 |
| **Al** (µg/L) | 42.7 | 8.51 | 8.61 | 52.0 | 55.5 | ND | 33.5 | 23.2 |
| **Alk** (mg/L $CaCO_3$) | 2425 | 4425 | 3030 | 4200 | 2200 | 2770 | 3175 | 929 |
| **EC** (mS/cm) | 29.8 | 29.2 | 33.2 | 33.1 | 34.8 | ND | 32.0 | 2.16 |
| **pH** | 7.28 | 10.9 | 9.56 | 14.2 | 14.3 | 11.2 | 11.2 | 2.71 |
| **TVS:TS** | 0.371 | 0.32 | 0.38 | 0.41 | 0.32 | 0.36 | 0.36 | 0.037 |
| **BOD:COD** | 0.30 | 0.32 | 0.18 | 0.28 | 0.26 | 0.27 | 0.27 | 0.054 |
| **C:N** | 8.94 | 5.48 | 5.06 | 3.58 | 2.64 | 2.48 | 4.70 | 2.41 |
| **VFA:Alk** | 1.09 | 0.70 | 1.38 | 0.64 | 0.91 | 0.97 | 0.95 | 0.30 |
| **COD: $SO_4^{2-}$** | 22.0 | 8.5 | 12.6 | 19.2 | 16.0 | 14.2 | 15.7 | 5.30 |
| **COD:TVS** | 2.12 | 2.07 | 1.92 | 1.15 | 2.13 | 2.23 | 1.94 | 0.40 |

ND = not determined, SD = standard deviation.

BOD:COD ratios of batch 4 and 5 of the TY (0.58 and 0.61, respectively), suggested that these batches contained a higher fraction of biodegradable organics (Table 1a) compared to BH with BOD:COD (≤ 0.32) (Table 1b) which suggested that BH had a higher fraction of inorganics and/or recalcitrant organics. Generally, BH processes are the main source of suspended (79%) and dissolved solids (61%), BOD (75%), and COD (75%) in TEs (Buljan and Král, 2019). In contrast to the BOD:COD ratio, the BH exhibited a higher TVS:TS (0.18–0.41) compared to TY (0.09–0.14). The TS, BOD and COD concentration ranges of all the batches were comparable to the ranges 10.1–31.5, 0.1–4.33, and 0.51–55 g/L reported in similar studies, respectively (Mpofu et al., 2021b). There is however limited literature on TOC, TVS, TS concentrations and TVS:TS ratios of TEs.

### 3.1.2. Concentration of nitrogen, carbon and volatile organic acids in the bovine/ovine tannery effluents

Expectedly, the total nitrogen (TN) concentrations of BH and TY batches were > 1000 mg/L, and > 500 mg/L, respectively. Unhairing contributes to the high nitrogen (N) and $HS^-$ content in BH (Table 6, Supplementary). These concentrations were notably higher than those reported in literature (112–915 mg/L) (Mpofu et al., 2021a). In contrast to TN in TE, which has been widely reported, only one literature report was found where TOC was included, and a few where C:N ratios were included as measured parameters (Mpofu et al., 2021a). The TOC concentrations of BH (3540–9250 mg/L, Table 1a) and TY (594–1330 mg/L, Table 1b) were higher than the 514 mg/L, reported in literature. The AD of TEs with low C:N ratios is susceptible to instability due to the potential accumulation of $NH_3$ and VOAs. Berhe and Leta (2018) reported C:N ratios between 6 and 9 as optimal for the AD of TE. The C:N ratios (2.49–8.94) of some BH batches were optimal, while those of TY (1.02–1.46) were below optimal, and therefore potentially susceptible to $NH_3$ inhibition during AD.

The total VOA ($VOA_t$) concentrations of BH (2.01–4.17 g/L) and TY (0.53–1.46 g/L) were mostly below the inhibitory thresholds reported in literature ($VOA_t$ = 5.80–6.90 g/L) ((Mpofu et al., 2021a). The VOA:ALK ratios of BH (0.64–1.38) and TY (0.11–0.73) were > 0.4, except for batch 2, 5 and 6 of TY. This indicated the likelihood of bioreactor instability and failure during AD (Gao et al., 2015). However, the speciation of $NH_3$–$NH_4^+$ and $CO_2$–$HCO_3^-$–$CO_3^{2-}$during AD serves as a buffer for maintaining pH within the optimal range.

### 3.1.3. Inorganic characteristics of bovine/ovine tannery effluents

The BH concentrations of nitrite ($NO_2^-$), nitrate ($NO_3^-$) and sulphide ($S^{2-}$) were higher than those of the TY, while their $NH_3$ and $Cl^-$ concentrations were comparable (ANOVA, $p > 0.05$). The $NH_3$ concentrations in all the batches were within the inhibiting range of 53–1450 mg/L reported in previous studies (Mpofu et al., 2021a). Beamhouse processes are the main source of inorganic

**Table 1b**
Characteristics of tanyard bovine/ovine tannery effluent.

| Parameter | Batch 1 | Batch 2 | Batch 3 | Batch 4 | Batch 5 | Batch 6 | Mean | SD ± |
|---|---|---|---|---|---|---|---|---|
| **TOC** (mg/L) | 930 | 594 | 1330 | 875 | 700 | 1208 | 940 | 285 |
| **COD** (mg/L) | 3880 | 4625 | 6570 | 1725 | 1955 | 4795 | 3925 | 1842 |
| **BOD** (mg/L) | 1500 | 1650 | 2443 | 900 | 1200 | 1800 | 1575 | 517 |
| **$VOA_t$** (mg/L AAE) | 1458 | 531 | 1985 | 1062 | 167 | 1102 | 1051 | 647 |
| **TN** (mg/L) | 765 | 580 | 910 | 545 | 595 | 980 | 729 | 185 |
| **TAN** (mg/L$NH_3$ – N) | 760 | 102 | 153 | 315 | 422 | 730 | 414 | 281 |
| **$NO_3$** (mg/L) | 0.70 | 0.61 | 0.80 | < 0.5 | 1.10 | 0.75 | 0.79 | 0.19 |
| **$NO_2$** (mg/L) | 0.01 | 5.5 | 5.65 | 0.30 | 0.32 | 0.34 | 2.01 | 2.76 |
| **TP** (mg/L $PO_4^{2-}$ – P) | 3.20 | 5.05 | 8.05 | 10.4 | 7.90 | 8.60 | 7.20 | 2.61 |
| **$SO_4^{2-}$** (mg/L) | 2740 | 4200 | 3400 | 2310 | 2090 | 2450 | 2865 | 796 |
| **$HS^-$** (mg/L) | 0.10 | 5.70 | 4.80 | 0.65 | 0.68 | 0.48 | 2.07 | 2.57 |
| **Cl** (mg/L) | 7725 | 7500 | 9400 | 2870 | 4620 | 7460 | 6595 | 2387 |
| **TS** (g/L) | 20.1 | 16.9 | 17.5 | 22.5 | 12.9 | 20.1 | 18.3 | 3.34 |
| **TVS** (g/L) | 2.34 | 1.50 | 2.51 | 2.02 | 1.29 | 1.79 | 1.91 | 0.47 |
| **Proteins** (mg/L) | 256 | 282 | 204 | 377 | 435 | 560 | 352 | 132 |
| **K** (mg/L) | 85.7 | ND | 80.3 | 105 | 130 | ND | 100 | 22.5 |
| **Na** (mg/L) | 6235 | ND | 6072 | 6664 | 5928 | ND | 6225 | 319 |
| **Fe** (mg/L) | 0.27 | ND | 0.04 | 0.34 | 0.11 | ND | 0.19 | 0.14 |
| **Ca** (mg/L) | 198 | ND | 212 | 331 | 183 | ND | 230 | 67.6 |
| **Mg** (mg/L) | 218 | ND | 215 | 263 | 186 | ND | 221 | 31.9 |
| **Zn** (µg/L) | 110 | ND | 78.6 | 189 | 383 | ND | 190 | 137 |
| **Cu** (µg/L) | 20 | ND | 25.1 | 22.6 | 236 | ND | 75.8 | 107 |
| **Co** (µg/L) | 0.00 | ND | 1.36 | 1.99 | 4.65 | ND | 2.00 | 1.95 |
| **Cd** (µg/L) | 0.00 | ND | 0.00 | 0.11 | 0.06 | ND | 0.04 | 0.05 |
| **Ni** (µg/L) | 20 | ND | 14.6 | 15.1 | 15.5 | ND | 16.3 | 2.5 |
| **Cr** (µg/L) | 130 | ND | 119 | 283 | 269 | ND | 200 | 87.7 |
| **Pb** (µg/L) | 0.00 | ND | 3.30 | 3.49 | 5.64 | ND | 3.11 | 2.33 |
| **Al** (µg/L) | 30 | ND | 15.0 | 25.3 | 42.0 | ND | 28.1 | 11.2 |
| **Alk** (mg/L $CaCO_3$) | 2010 | 1730 | 2705 | 1960 | 1590 | 5420 | 2569 | 1449 |
| **EC** (mS/cm) | 31.4 | ND | 31.1 | 33.9 | 29.4 | ND | 31.5 | 1.59 |
| **pH** | 8.38 | 8.80 | 8.52 | 8.04 | 8.48 | 7.82 | 8.34 | 0.35 |
| **TVS:TS** | 0.12 | 0.09 | 0.14 | 0.09 | 0.10 | 0.09 | 0.11 | 0.02 |
| **BOD:COD** | 0.39 | 0.36 | 0.37 | 0.52 | 0.61 | 0.38 | 0.44 | 0.11 |
| **C:N** | 1.22 | 1.02 | 1.46 | 1.61 | 1.18 | 1.23 | 1.29 | 0.21 |
| **VFA:Alk** | 0.73 | 0.31 | 0.73 | 0.54 | 0.11 | 0.20 | 0.44 | 0.27 |
| **COD:$SO_4^{2-}$** | 4.17 | 7.79 | 4.94 | 1.97 | 2.79 | 3.97 | 4.27 | 2.02 |
| **COD:TVS** | 1.66 | 3.09 | 2.62 | 0.85 | 1.51 | 2.67 | 2.07 | 0.86 |

ND = not determined, SD = standard deviation.

substances such as nitrogen compounds (85%), and sulphide (80%) in BOTE (Buljan and Král, 2019).

There were significant batch-to-batch $SO_4^{2-}$differences (ANOVA, $p < 0.05$) which were assumed to emanate mainly from the tanning operations. As expected, TY batches exhibited higher $SO_4^{2-}$ concentrations (2090–4200 mg/L) than BH (1120–2400 mg/L) as chrome sulphate [$Cr_2(SO_4)_3$] is used as a tanning agent. These were comparable to the 450–3900 mg/L concentration range from previous studies (Mpofu et al., 2021a). According to Buljan and Král (2019), TY and BH are expected to contribute 16% and 52% $SO_4^{2-}$ to final TE emissions. The COD: $SO_4^{2-}$ ratios (5.3–22) of BH batches were likely to favour methanogenesis, while those of TY (0.75–1.96) were likely to support sulfidogenesis (Chou et al., 2008). Nonetheless, the $HS^-$ levels in BH (276–476 mg/L) were inhibitory to methanogens and sulfidogenesis was likely to be favoured. The $IC_{50}$ ranges for $H_2S$ determined by O'Flaherty et al. (1998) for methanogenic archaea were 43–125 mg/L at pH 7–8, 57–184 and 14–60 mg/L at pH 7.2–7.4 and 8.0–8.5 for aceticlastic methanogens (AMs), respectively.

### 3.1.4. Metal profiles

The metal concentrations of BH and TY batches displayed similar trends ($r = 0.73–0.99$, F test, $p < 0.05$) except for Ni, Pb and Cr. The total Cr concentration range was 39–283 µg/L and was on the lower end of the 0.26–7000 mg/L concentration range from literature (Mpofu et al., 2021a). As was expected, concentrations of K (45.6–129 and 85.7–130 mg/L), Na (5.55–7.18 and 5.93–6.66 g/L), Ca (0.2–1.42 and 0.18–0.33 g/L) and Mg (3.7–375 and 186–263 mg/L) in BH and TY, respectively, were equally high as they are added in different forms to preserve skin/hides and/or throughout the tanning process. These concentrations ranges were comparable to the 0.14–17.4 g/L Na, 0.06–2.98 g/L Ca, and 3.19–48 mg/L Mg reported in previous studies (Mpofu et al., 2021a). There is a lack of studies reporting on the metal concentrations in TEs. Metabolic co-factors Ni, Zn, Co, Cu and Ca were either within or below the optimal literature range for AD (Mpofu et al., 2021a).

Nonetheless, a wide range of inhibitory concentrations of metals have been reported in literature due to variability in bacterial acclimation, substance synergism, and antagonism on different reactor operating conditions (Mpofu et al., 2021b), and the fact that microbial communities may adapt and prevent metal toxicity or deficiency (Thanh et al., 2016). The full scale application of this study is expected to succeed provided the versatile microorganisms and optimum operational parameters are maintained (Kibangou et al., 2021). Based on the inhibitory concentrations reported in literature,

**Table 2**
Experimental design matrix showing the gas yields and biodegradability results.

| Reactor | A:Composition BH | B:ISR | Biogas Yield | Methane Yield | Average Methane | Biodegradability indicators (% Reduction) | | | | |
|---|---|---|---|---|---|---|---|---|---|---|
| | | | | | | TOC | Sulphate | TS | VS | COD |
| | (%) | | (mL/gVS) | (mL/gVS) | % | (%) | (%) | (%) | (%) | (%) |
| R1 | 50 | 2.5 | 473 | 196 | 41 | 51.8 | 37.1 | 32.2 | 46.0 | 67.4 |
| R2 | 25 | 2.0 | 139 | 25 | 18 | 56.7 | 68.0 | 16.9 | 18.9 | 49.0 |
| R3 | 75 | 3.0 | 600 | 218 | 36 | 37.7 | 38.8 | 26.0 | 34.3 | 65.9 |
| R4 | 50 | 2.5 | 415 | 161 | 39 | 42.0 | 63.3 | 32.5 | 49.3 | 64.7 |
| R5 | 0 | 2.5 | 0 | 0 | ND | 29.3 | 40.5 | 19.6 | 34.8 | 55.3 |
| R6 | 50 | 1.0 | 57 | 7.6 | 13 | 13.1 | 44.5 | 17.9 | 29.7 | 12.3 |
| R7 | 75 | 2.0 | 0 | 0 | ND | 44.2 | 58.9 | 29.9 | 42.8 | 70.2 |
| R8 | 100 | 2.0 | 692 | 357 | 52 | 39.3 | 53.9 | 37.6 | 52.5 | 68.4 |
| R9 | 50 | 2.5 | 460 | 162 | 39 | 56.0 | 53.7 | 30.3 | 44.7 | 64.6 |
| R10 | 50 | 4.0 | 296 | 79 | 27 | 29.8 | 45.2 | 30.6 | 42.2 | 50.2 |
| R11 | 25 | 3.0 | 153 | 39 | 25 | 37.9 | 84.6 | 25.4 | 36.7 | 84.4 |
| R12 | 50 | 2.5 | 440 | 173 | 39 | 25.5 | 65.9 | 28.0 | 46.1 | 68.8 |
| R13 | 50 | 2.5 | 329 | 120 | 36 | 58.8 | 69.5 | 27.3 | 45.7 | 64.3 |
| R14 | 100 | 3.0 | 393 | 150 | 38 | 12.2 | 75.0 | 13.4 | 45.6 | 62.5 |
| R15 | 100 | 4.0 | 257 | 89.7 | 35 | 17.0 | 37.1 | 24.7 | 54.5 | 57.0 |
| R16 | 0 | 2.0 | 0 | 0 | ND | 45.3 | 48.9 | 17.1 | 24.3 | 65.5 |
| R17 | 0 | 4.0 | 0 | 0 | ND | 21.9 | 33.5 | 33.9 | 49.5 | 47.8 |

COD = chemical oxygen demand, Conc = concentration, ISR = inoculum to substrate ratio, R = reactor, TOC = total organic carbon, TS = total solids, VS = volatile solids.

Na in BH and TY (Tables 1a and 1b) was within the inhibitory range whereas other metals were below the inhibitory range reported by previous studies (Mpofu et al., 2021a).

### 3.2. Optimisation of anaerobic biodegradability and resource recovery

The experimental $CH_4$ (0–357 mL/gVS) and biogas (0–692 mL/gVS) yields and $B_o$ [% reduction TOC (12.2–58.8%), $SO_4^{2-}$ (33.5–84.6%), COD (12.3–84.4%), VS (18.9–52.5%), and TS (16.9–37.6%) (Table 2) were modelled using a general quadratic polynomial with up to second degree interaction terms, and linear equations (Table 3 and Fig. 1).

The fractional design space (FDS = 0.99) and the signal:noise ratios were sufficiently greater than the recommended 0.8, while the adequate precision for all the empirical models were desirably > 4 (Stat-Ease, Inc., Minneapolis, USA). The F test showed that BH composition was a significant ($p < 0.05$) model term for gas yield (biogas and $CH_4$) and $B_o$ (%TS and %TOC reduction), whereas ISR and its interactions [$(ISR)^2$ and (%BH comp)(ISR)] were the only significant terms (F test, $p < 0.05$) on %TS and %COD reduction, respectively. However, both terms were not significant on $B_o$ ($\%SO_4^{2-}$, % VS and %TOC reduction) as all the reactors were somewhat active.

All the models were significant (F test, $p < 0.05$), and there was only 0.01–4.0% chance that this may have occurred due to noise (Table 3). The correlation coefficients ($R^2$) of the models (Table 3) indicated that 53; 49; 35% and 5% of the variability in biogas yield, $CH_4$ yield, %TS and %COD reduction was not explained by the models, respectively. The models' adj. $R^2$ values which corrected the $R^2$ values with respect to the sample size and number of terms in the models were 0.58 and 0.93 for %TS and %COD reduction, suggesting the models' moderate and good predictability, respectively. The high variability in biogas and $CH_4$ yields (adj. $R^2$ = 0.37 and 0.41, respectively) was an indication of the complexity of reactor contents, consortium and the biochemical reactions that were taking place leading to gas production.

The general quadratic polynomial and linear equations (Eqs. 1–7) generated by Design-Expert® Software Version 10 (Stat-Ease, Inc., Minneapolis, USA) were statistically tested for significance and their accuracy in fitting the experimental data of gas yields and $B_0$ (Table 3). The $CH_4$ yield, %COD and %VS reduction models (Eqs. 2, 4 and 6) did not fit the data very well (Lack of fit: F test, $p \leq 0.05$) (Table 3). Therefore, excluding these three, other models (Eqs. 1, 3, 5, 6 and 7) were used to navigate the design space and to optimise the cumulative biogas yields, TOC, $SO_4^{2-}$, and %TS reduction as plotted in Fig. 1. Based on the interest to maximise gas yields and $B_o$, the theoretical optimum operating conditions were found to be at 100% BH composition and ISR = 2.5, with a desirability of 0.73. These optimum conditions were expected to generate 562 mL biogas/gVS, 262 mL$CH_4$/gVS, with reduction efficiencies of 40.8%, 55.7%, 67.6%, 49.4%, and 35.6%, for TOC, $SO_4^{2-}$, COD, VS, and TS, respectively.

$$\textbf{Biogas yield} = \mathbf{121ISR + 5.64\%Comp - 308} \quad (1)$$

$$\mathbf{CH_4\ yield} = \mathbf{3.13ISR^2 + 0.01(\%Comp)^2 0.05ISR - 55.4} \quad (2)$$

**Table 3**
Summary of the statistical results of the fitted models.

| Models | Std dev | p-value | F test (LOF) p value | $R^2$ | Adj $R^2$ | Adeq Prec | AIC |
|---|---|---|---|---|---|---|---|
| Biogas Linear | 189 | 0.04 | 0.55 | 0.47 | 0.37 | 6.21 | 178 |
| $CH_4$ Linear | 2.99 | 0.03 | 0.01 | 0.51 | 0.41 | 6.91 | 70.6 |
| TOC Quadratic | 0.03 | 0.01 | 0.61 | 0.63 | 0.55 | 8.73 | -52.5 |
| Sulphate Mean | ND | ND | 0.42 | ND | ND | ND | 107 |
| TS Linear | 3.97 | 0.01 | 0.10 | 0.65 | 0.58 | 8.67 | 78.0 |
| VS 2FI | 0.17 | 0.05 | 0.001 | 0.56 | 0.42 | 6.08 | -0.32 |
| COD Quadratic | 4.66 | < 0.0001 | 0.03 | 0.95 | 0.93 | 22.4 | 89.2 |

Adeq Prec=adequate precision, Adj=adjusted, AIC=Akaike's Information Criterion, LOF=lack of fit, COD=chemical oxygen demand, ND=not determined, Pred=predicted, Std dev=standard deviation, TS=total solids, TOC=total organic carbon, VS=volatile solids.

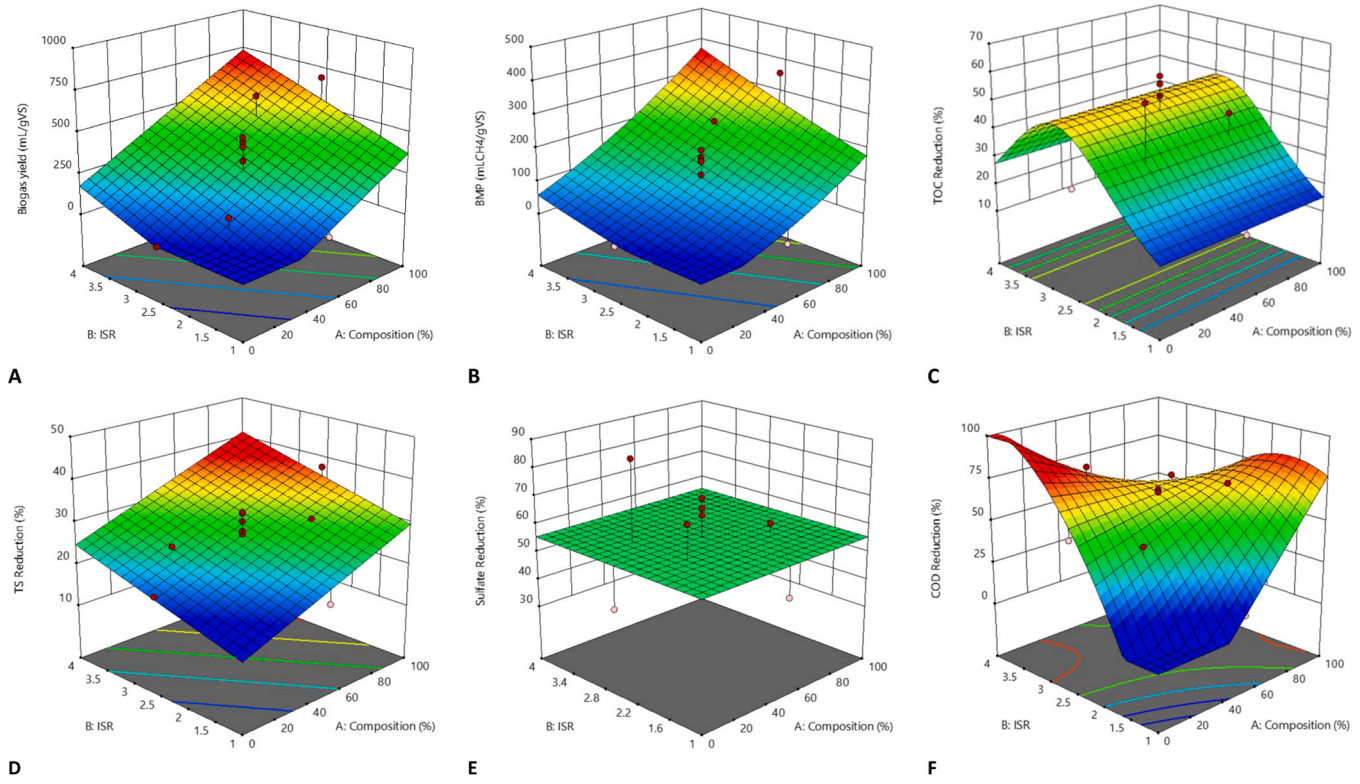


**Fig. 1.** Effect of BH concentration and inoculum to substrate ratio on: A – biogas yield; B – cumulative methane yield; C – total organic carbon reduction; D – total solids reduction; E – sulphate reduction; and F – COD reduction during anaerobic co-digestion of segregated b/ovine tannery effluents.

$$\%\,\mathbf{TOC_{reduction}} = \frac{\mathbf{1}}{\mathbf{0.176 - 0.04ISR^2 + 0.001ISR^4}} \quad (3)$$

$$\%\,\mathbf{VS_{reduction}} = \mathbf{1.04\%Comp + 2.33ISR - 1.01Comp(ISR) - 1.61} \quad (4)$$

$$\%\,\mathbf{TS_{reduction}} = \mathbf{3.88ISR + 0.16\%Comp + 9.27} \quad (5)$$

$$\%\,\mathbf{COD_{reduction}} = \mathbf{-15.4ISR^2 - 0.79\%Comp(ISR) + 130ISR + 2.08\%Comp - 167} \quad (6)$$

$$\%\,\mathbf{SO_{4reduction}} = \mathbf{55.7} \quad (7)$$

### 3.2.1. Biomethane recovery

The repeat experiments to confirm the theoretical optimum conditions yielded 639 mL biogas/gVS, 377 mL $CH_4$/gVS (59% average $CH_4$), with reduction efficiencies of 42.2%, 57.8%, 62.6%, 64.5%, and 48.3%, for TOC, $SO_4^{2-}$, COD, VS, and TS, respectively. The optimum COD removal (62.6%) was comparable to the 43–95% removal efficiencies reported by previous studies (Mpofu et al., 2021a). The cumulative $CH_4$ yields were higher than optimum yields obtained by Saxena et al. (2019), Berhe and Leta (2018) and Mpofu et al. (2021b) for AD of general TEs with and/or without pre-treatment (7.6–27 mL/gVS, 56–61 mL/gCOD, and 0–146 mL/gVS after 35, 20, and 52 days, respectively. These results were also lower than the 406–753 mL$CH_4$/gVS and comparable to the 653–737 mL biogas/gVS determined by Achouri et al. (2017) after 37 days. Achouri et al. (2017) reported higher $CH_4$ quality (%v/v) of 53–84% presumably due to the higher dilutions (34–53%) using tap water, addition of optimal micronutrients, and use of a blend 50:50 (v/v) of BH and a combination of TY and dye house effluents at ISR = 1.5. The 13–59% average $CH_4$ quality measured in this study was due to parallel reactions that produced other gases such as $CO_2$, CO, $H_2S$, and other gases that could not be quantified using the biogas 5000 analyser. It was theorised that the main gas was most likely $N_2$ (Eqs. 8–15), and the rest of the gases were $NH_3$, $H_2$ and/or VOAs produced by AD processes. Nonetheless, the $CH_4$ yields from this study were comparable to 261–437 and 314 mL/gVS reported by Vazifehkhoran et al. (2018) while co-digesting general TWW with cleaning (drainage) effluent and wheat straw (1:9 w/w) at ISR = 3, respectively.

The performance of the reactors improved with increasing %BH composition and up to ISR = 3 ( Fig. 2 A–D). At ISR > 3 reactor performance decreased significantly at all %BH compositions. This strongly suggested that the characteristics of BH were more suitable for AD than TY, notably due to lower concentration of toxicants, and higher concentrations of essential macro- and micro-nutrients (Tables 1a and 1b). The inhibition of reactors that led to the long lag phases and lack of $CH_4$ production is discussed in Section 3.3. In practical terms, these results suggest that bioreactors must be operated at 100% BH and ISR ($2 \leq ISR \leq 3$) by optimising the solids retention time (SRT) and/or desludging rate. Fig. 2

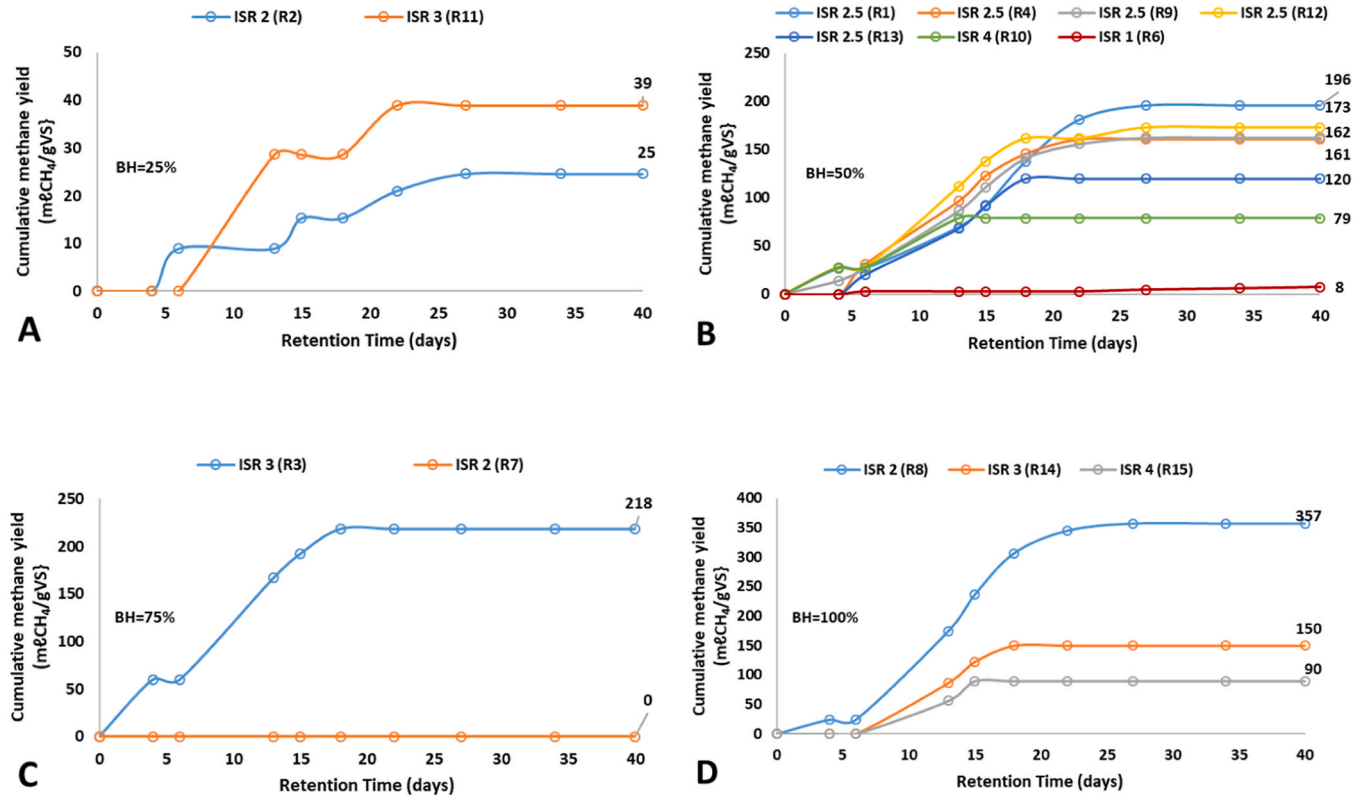


**Fig. 2.** Cumulative methane yields of reactors operating at different inoculum to substrate ratios (A-D) and beamhouse effluent composition: 25% (A), 50% (B), 75% (C), 100% (D).

*3.2.1.1. Kinetic study of cumulative methane production*. The fitted models displayed perfect fit to the experimental data with high precision and suitability [F test, $p < 0.05$ and $0.823 \leq \text{Adj } R^2 \leq 0.999$). The models fitted the cumulative $CH_4$ production data in the order: Logistic > modified Gompertz > Cone > Chen and Hashimoto > First order ( Fig. 3); (Table 7, Supplementary). According to the statistical parameters (Table 7, Supplementary), the first order ($0.823 \leq \text{Adj } R^2 \leq 0.950$) and the Chen and Hashimoto (C&H) models ($0.825 \leq \text{Adj } R^2 \leq 0.970$) were the worst predictors of cumulative $CH_4$ yields of most reactors. This was unexpected as all the reactors experienced none to shorter lag phases (0–6 days) and the exponential rise to a maximum curve portrayed by the first order model should have accurately fitted the data. However, the inhibition of microbial activity affected the proportionality between $CH_4$ production and substrate depletion. Mpofu et al. (2021b) also reported the first order model as the overall worst performer, particularly for all the reactors that experienced a lag phase and the best fit for reactors that did not experience any lag phase.

The Logistic, Cone and modified Gompertz model were the best performers ($0.827 \leq \text{Adj } R^2 \leq 0.999$) for most reactors as they assume proportionality between $CH_4$ production and microbial activity or growth rate which is proportional to inhibition. Additionally, the models resemble a sigmoidal shape (Fig. 3) which is adequate for predicting the lag phase, and exponential rise to a maximum. This was the case in this study as: (i) the proportion of BH detected the initial amount of biodegradable substances added into the reactor; (ii) the amount of stimulating or inhibiting substances, and (iii) the initial reactor ISR determined the starting microbial population.

The highest $CH_4$ production rates ($\mu_m$) were found in reactors R8, R14 and R15 operating at 100% BH and ISR = 2, 3 and 4 respectively, while highest reaction rate constants (K) were found in R3 and R10 operating at 50% and 75% BH and ISR = 3 and 4, respectively. These results confirm that from the range of parameters tested, higher % BH and ISR ≥ 3 provided the most ideal environment for proliferation of methanogens. The $\mu_m$ = 0.04–74.2 $mLCH_4/gVSd$ and K = 0.06–0.16 $day^{-1}$ results in this study were somewhat comparable to $\mu_m$ = 0.171–17.5 $mLCH_4/gVSd$ and K = 0.025–0.268 $day^{-1}$ reported by Mpofu et al. (2021b), while digesting slaughterhouse-ostrich TE. The authors reported that the kinetics from their study were higher than those reported while co-digesting tannery sludge with other organic solid wastes. Nonetheless, there is a lack of studies investigating reaction kinetics during AcoD of TWW. Fig. 3.

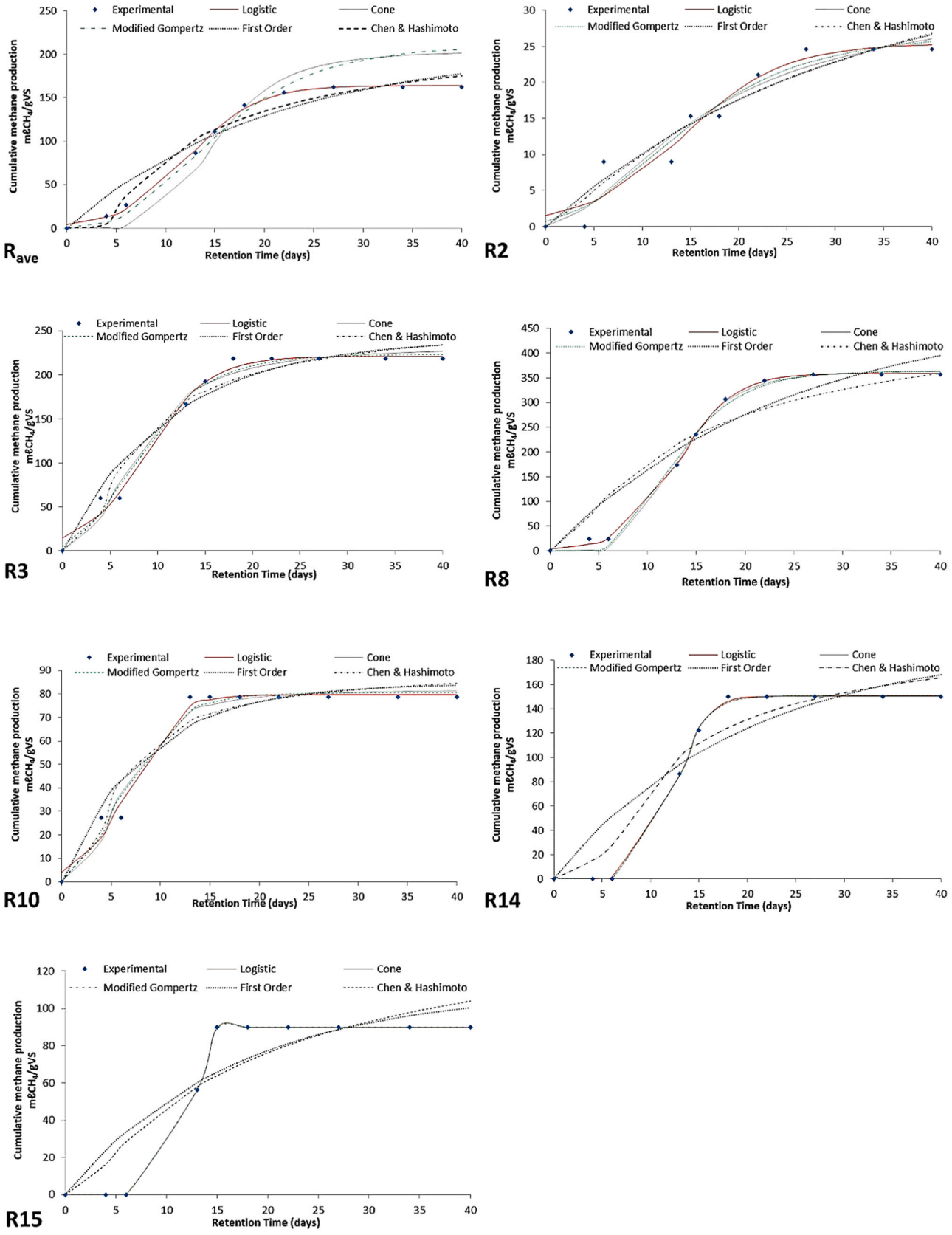


**Fig. 3.** Graphs depicting the experimental and model curves for cumulative methane yields during the anaerobic co-digestion of beamhouse and tanyard b/ovine tannery effluents at different operating conditions: $R_{ave}$–50%BH, ISR = 2.5; R2–25%BH, ISR = 2; R3–75%BH, ISR = 3; R8–100%BH, ISR = 2; R10–50%BH, ISR = 4; R14–100%BH, ISR = 3; and R15–100% BH, ISR = 4.

*3.2.2. Sulphur recovery*

It was apparent that at least a fraction of the $HS^-$ formed from sulfidogenesis was oxidised into elemental sulphur ($S_0$). A white yellowish layer was formed at the interface of the bulk liquid and head space in the reactors. White yellowish flakes were also observed settling to the bottom of the reactors and were most apparent in R5, R7, R8, R11, and R16 that operated at higher/lower BH composition (0%, 75%, 100%, 25%, and 0%) and ISR ≤ 3 (2.5, 2.0, 2.0, 3.0, and 2.0), respectively. These reactors also suffered methanogenesis inhibition as they had high initial $SO_4^{2-}$ concentrations that supported sulfidogenesis. Chemolithotrophic sulphur oxidising bacteria (SOB) can facilitate the formation of $S_0$ from the oxidation of $HS^-$ and $H_2S$ by nitrate ($NO_3^-$) and nitrite ($NO_2^-$) during AD following the reactions in Eqs. 8–11 (Moraes et al., 2012). The consumption of $H^+$ by SOB could explain the anomalous increase in alkalinity in some reactors (Section 3.3.1). The biological formation of $S_0$ presents an ideal opportunity for $S_0$ and nitrogen gas ($N_2$) recovery from TE.

$$\mathbf{5HS^- + NO_3^- + 3H^+ \rightarrow 5SO_4^{2-} + 4N_2 + 4H_2O} \quad (8)$$

$$\mathbf{3HS^- + 8NO_2^- + 5H^+ \rightarrow 3SO_4^{2-} + 4N_2 + 4H_2O} \quad (9)$$

$$\mathbf{5HS^- + 2NO_3^- + 7H^+ \rightarrow 5S_0 + N_2 + 6H_2O} \quad (10)$$

$$\mathbf{3HS^- + 2NO_2^- + 5H^+ \rightarrow 3S_0 + N_2 + 4H_2O} \quad (11)$$

A notable $NO_3^-$ decrease (7–81%) in all reactors performing mono AD of TY or BH effluent and in the severely or permanently inhibited reactors supported the hypothesis that it was readily utilised as an electron donor by SOB. This confirmed the conspicuous accumulation of $S_0$, $NO_2^-$ (10–133%) and utilisation of $HS^-$ particularly in reactors that operated at higher/lower BH composition (0%, 25%, 75% and 100% BH) and ISR ≤ 3. The accumulation of $NO_2^-$ may have partly inhibited methanogenesis (Moraes et al., 2012). It is also possible that the observed $NH_4^+$ accumulation was partly due to dissimilatory process of $NO_3^-$ reduction to $NH_4^+$ on top of protein hydrolysis. However, $NO_3^-$ accumulation in the rest of the reactors (12–255% increase) suggested occurrence of nitrification by microorganisms responsible for anaerobic ammonium oxidation (ANAMMOX). Whereas, in R2 (25%BH and ISR = 2) and R9 (50%BH and ISR = 2.5) it coincided with 13% and 46% $NO_2^-$ reduction respectively, as it may have been used as the preferred electron donor over $NO_3^-$ for $HS^-$ oxidation.

ANAMMOX reactions (Eqs. 12–15) may have been a contributing pathway for $S_0$ and $N_2$ formation. These reactions were also postulated by Sabumon (2008a, 2008b) whom injected air at the bottom of the reactor and observed the formation of $S_0$ from the oxidation of $HS^-$ and $H_2S$ in the anoxic region of an up-flow hybrid reactor treating primary treated blended TE. The author also reported that 20–23% of the inlet sulphur escaped in treated TE while 63–66% was recovered as $S_0$. Mpofu et al. (2021b) observed the possibility of producing $S_0$ during AD of ostrich TE combined with slaughterhouse effluent. The authors also observed re-formation of $SO_4^{2-}$, ostensibly from the anaerobic oxidation of $S_0$ by $NO_3^-$ and/or $NO_2^-$. However, the dominant pathway for $S_0$ production was not postulated. A sulphur mass balance on reactors operating at optimum conditions indicated that about 13% of influent sulphur is recoverable as $S_0$, 12% in the sludge and 22% in biogas, while 53% escapes in the effluent. Sabumon (2008a, 2008b) achieved higher $SO_4^{2-}$ removal (64.2–83.1%) and $S_0$ recovery (63–66%) as a sulfidogenic culture was used and oxygen (air) was added while limited $NO_3^-$ and $NO_2^-$ acted as oxidising agents in this study. The recovered $S_0$ can be harvested by skimming or retrofitting the batch reactor with a fine mesh filter. Work by Kibangou et al. (2021) on the AcoD of TE and slaughterhouse wastewater demonstrated the preferential selection of metabolically versatile methanogenic genus *Methanosarcina spp*, *Methanobacterium*, and *Methanosaeta* in both unmixed and continuously mixed reactor regimes. They further reported *Desulfovibrio*, *Desulfomicrobium*, *Desulfobacterium* and a member of the order *Clostridiales* as the most abundant SRB genera in both reactor regimes. Similar to this work, their work demonstrated the syntrophic coexistence of SRB and methanogens.

$$\mathbf{3SO_4^{2-} + 4NH_4^+ \rightarrow 3S^{2-} + 4NO_2^- + 4H_2O + 8H^+} \quad (12)$$

$$\mathbf{3S^{2-} + 2NO_2^- + 8H^+ \rightarrow 3S_0 + N_2 + 4H_2O} \quad (13)$$

$$\mathbf{2NO_2^- + 2NH_4^+ \rightarrow 2N_2 + 4H_2O} \quad (14)$$

$$\mathbf{SO_4^{2-} + 2NH_4^+ \rightarrow S_0 + N_2 + 4H_2O} \quad (15)$$

Nonetheless, the autotrophic denitrification and anaerobic ammonia nitrification integrated with sulphide oxidation occur via complex biochemical reactions that depend on various factors and the dominant pathway/s (species) were inconclusive in this study. Microbial analysis must be conducted in future studies to ascertain the dominant species and biochemical pathways. It was therefore hypothesised that (i) sulfidogenesis, methanogenesis, anaerobic ammonia oxidation and mixotrophic denitrification occurred concurrently, and (ii) sulfidogenesis initially dominated, followed by methanogenesis (particularly hydrogenotrophic) in the active reactors. This was supported by qualitative analysis of the biogas which showed very low $\%CO_2$ compared to $\%CH_4$ ($CH_4$: $CO_2 > 1$) and high $H_2S$ > 1610–9999 ppm during the first 2–6 days hydraulic retention time (HRT), which gradually increased over time. Further research is needed to maximise sulphur production as a pretreatment step to remove sulphide using a modified bioreactor such as the hybrid linear flow channel reactor to make BOTE more amenable for AD (Marais et al., 2020).

*3.2.3. Nitrogen recovery*

The final $NH_3$ concentrations in the soluble fraction (filtrate) in all the reactors ranged from 264 to 596 mg/L. The TE can be recycled and further processed downstream to recover nitrogen as a fertiliser. This could be accomplished by adding Mg and P to precipitate struvite ($MgNH_4PO_4.6H_2O$), or through $NH_3$ stripping. Additional downstream ANNAMOX can be employed to further remediate the anaerobically treated BH and convert the $NH_3$ to $N_2$. However, sustainable and economically feasible options must be explored. A mass balance on nitrogen suggested that the optimal reactor conditions recovered about 18% of the influent nitrogen as $N_2$ in biogas. The $CO_2$ and $N_2$ in the biogas most likely resulted from the autotrophic denitrification and/or ANNAMOX integrated with sulphide oxidation (Eqs. 8–15) can be recovered through absorption and stripping. Pilot studies will focus on using gas chromatography to ascertain biogas constituents.

*3.2.4. Water reuse*

Apart from recycling the treated BOTE for $N_2$ or $NH_3$ recovery, it can be used for irrigation purposes. The treated BOTE characteristics met the stipulated irrigation standards of various developing countries that lead in bovine leather production (Table 4). The treated BOTE did not meet the discharge standards for Na, Mg, B, Cr, Cl, nitrogen, and $NH_3/NH_4$ in many of the countries (Table 4). In the South African context, the treated BOTE characteristics met the discharge standards for irrigating up to 500 $m^3$/day (Department of Water Affairs, 2013). This is suitable for a medium sized tannery processing about 100 tonnes/day of raw bovine hides (Swartz et al., 2017). Nonetheless, the BOTE can be mixed with other water sources to meet the 2000 $m^3$/day irrigation standards for COD (75 mg/L), Cl (0.25 mg/L), phosphorous (10 mg/L), nitrogen (15 mg/L) and $NH_3$ (3.0 mg/L). Maqbool et al. (2018) reported 50:50 (v/v) of TE and tap water as optimal for irrigating vegetables. Additionally, it can be further treated and/or diluted for reuse within the tanning process e.g. in soaking, de/liming and/or tanning (Buljan and Král, 2019).

**Table 4**
Allowable limits for wastewater and sludge for agriculture application in leading bovine leather producing countries including South Africa.

| Country | Brazil | China | Egypt | Ethiopia | India | Mexico | South Africa | South Korea | Turkey | Limit Range | This study (range) |
|---|---|---|---|---|---|---|---|---|---|---|---|
| pH | 6–9\|ND | 5.5–8.5\| ND | ND=ND | ND=ND | 5.5–9.0\|ND | 5–10\|ND | 5.5–9.5\|ND | 5.5–8.5\|ND | 6–9\|ND | 5.5–9.5\|ND | 7.76–8.52\|ND |
| (TSS)/TDS | 450–2000\|ND | (60–100)/2000\|ND | 20–250\|1000 | ND=ND | (200)/2100\|ND | 20–30\|ND | 25\|ND | ND=ND | (20–60)\|ND | (20–100)/20–2100\|ND | ND= 5.9–12.9 |
| COD | ND=ND | 40–200\|ND | ND=ND | 500\|ND | ND=ND | ND=ND | 75–400\|ND | ND=ND | ND=ND | 40–500\|ND | 270–3310\|ND |
| $BOD_5$ | 60–120\|ND | 40–100\|ND | 20–400\|ND | 200\|ND | 100\|ND | 20–30\|ND | ND=ND | 8.0\|ND | 0–200\|ND | 8–400\|ND | ND=ND |
| ($\mathbf{NO_3}$)/TN | /20–70\|ND | ND=ND | ND=ND | (50)/60\|ND | ND=ND | ND=ND | 15\|ND | ND=ND | (0–50)\|ND | (0–50)/15–70\|ND | (0.3–7.1)/321–551\|ND |
| Coliform | ND=ND | 2000–40000\|ND | 1000–5000\|ND | ND=ND | ND=ND | 1000\|1000 | 100–100000\|ND | 200\|ND | 0–1000\|ND | 100–100000\|ND | ND=ND |
| $\mathbf{NH_3}$/$\mathbf{NH_4}$ | ND=ND | ND=ND | ND=ND | 30\|ND | ND=ND | ND=ND | 3.0\|ND | ND=ND | 0–50\|ND | 0–50\|ND | 256–596\|ND |
| TP | 4–30\|ND | ND=ND | 30\|ND | ND=ND | ND=ND | ND=ND | 10\|ND | 0.2–2.0\|ND | ND=ND | 0.2–30\|ND | 6.5–20.8\|4569–7290 |
| EC | 0.5–2.7\|ND | ND=ND | ND=ND | ND=ND | ND=ND | ND=ND | 70–200\|ND | 0.7–2.0\|ND | 0–3\|ND | 0.5–200\|ND | ND=ND |
| Se | 0.02–0.05\|100 | 0.02\|ND | 0.02\|36 | ND=ND | ND=ND | ND=ND | ND=ND | 0.02\|ND | 0.02\|ND | 0.02–0.05\|36–100 | ND= 0.89–2.15 |
| Mo | ND= 40 | 0.05\|ND | 0.01\|18 | ND=ND | ND=ND | ND=ND | ND=ND | ND=ND | 0.01\|ND | 0.01–0.05\|18–40 | ND= 6.88–12.4 |
| As | 0.05–1.0\|51 | 0.05\|75 | 0.1\|41 | ND=ND | 0.2\|10 | 0.4\|41–75 | ND=ND | 0.05\|50 | 0.1\|ND | 0.05–0.4\|10–75 | ND= 1.64–6.63 |
| Cd | 0.01\|39 | 0.01\|5–20 | 0.01\|39 | ND=ND | ND= 5 | 0.1\|39–85 | ND= 40–85 | 0.01\|30 | 0.01\|3 | 0.01–0.1\|3–85 | ND= 0.27–0.71 |
| Cu | 0.2–1.0\|1500 | 1.0\|800–1500 | 0.2\|1500 | ND=ND | ND= 300 | 6.0\|1500–4300 | ND= 1500–4300 | 0.2\|500 | 0.2\|450 | 0.2–6.0\|300–4300 | 0–0.34\|167–333 |
| Hg | 0.002\|17 | 0.001\|5–15 | 0.002\|17 | ND=ND | ND= 0.15 | 0.01\|17–57 | ND= 15–55 | 0.001\|40 | ND= 5 | 0.001–0.01\|0.15–57 | ND= 1.86–50.0 |
| Ni | 0.2–0.5\|40 | 0.1\|100–200 | 0.2\|420 | ND=ND | ND= 50 | 4.0\|420 | ND= 420 | 0.2\|ND | ND= 120 | 0.1–4.0\|40–420 | 0.09–0.59\|18.5–32.9 |
| Pb | 0.1–5.0\|300 | 0.2\|300–1000 | 5.0\|300 | ND=ND | ND= 100 | 10\|300–840 | ND= 300–840 | 0.1\|1000 | 5.0\|150 | 0.1–10\|150–1000 | 0.0\|18.8–35.6 |
| Zn | 2–5\|2800 | 2.0\|2000–3000 | 5.0\|2800 | ND=ND | ND= 1000 | 20\|2800–7500 | ND= 2800–7500 | 2.0\|ND | 2.0\|1100 | 2–20\|1000–7500 | 0.08–0.75\|1620–2870 |
| Ca | 80–400\|ND | ND=ND | 230\|ND | ND=ND | ND=ND | ND=ND | ND=ND | ND=ND | ND=ND | 80–400\|ND | 93–341\|31746–76873 |
| Mg | 50–120\|ND | ND=ND | 100\|ND | ND=ND | ND=ND | ND=ND | ND=ND | ND=ND | ND=ND | 50–120\|ND | 71–583\|2668–5413 |
| Cr | 0.05–0.1\|1300 | 0.1\|ND | 0.1\|1200 | 2\|ND | ND= 50 | 1.0\|1200–3000 | ND= 1200–3000 | 0.05\|30 | 0.1\|350 | 0.05–2\|50–3000 | 0.42–1.86\|2803–6950 |
| Fe | 0.2–5\|ND | 1.5\|ND | 5.0\|ND | ND=ND | ND=ND | ND=ND | ND=ND | ND=ND | 5.0\|ND | 0.2–5.0\|ND | 0.67–2.89\|1243–2707 |
| B | 0.5–3.0\|ND | 1.0\|ND | 1.0\|ND | ND=ND | 2.0\|ND | ND=ND | ND=ND | 0.75\|ND | 0–2.0\|ND | 0.5–3.0\|ND | 1.58–7.03\|47.3–83 |
| Cl | 70–530\|ND | 350\|ND | 400\|ND | 1000\|ND | 600\|ND | ND=ND | 0.25\|ND | ND=ND | 0–710\|ND | 0–1000\|ND | 2050–6900\|ND |
| $\mathbf{SO_4}$/S | 100–1000\|ND | ND=ND | 500\|ND | /1\|ND | 1000\|ND | ND=ND | ND=ND | ND=ND | 0–960\|ND | 0–1000\|ND | 75–785\|ND |
| Na | 50–70\|ND | ND=ND | 230\|ND | ND=ND | #60\|ND | ND=ND | ND=ND | ND=ND | #20–80\|ND | 50–230\|ND | * 2.73–18.9\|6.58–41.8 |
| Reference | **1; 2** | **1; 2; 3** | **2;3;4** | **2; 10** | **5** | **1**; **2**; **7** | **2; 8; 9** | **9;10** | **2; 11** | | |

Water (mg/L)|sludge (mg/kg), * water (g/L)| sludge (g/kg), # (%), pH (dimensionless), EC=electrical conductivity ($mSm^{-1}$), Coliform (cfu/100 mL), ND=not determined, TDS=total dissolved solids, T/SS=total suspended solids, (De Morais Ferreira et al., 2019)[1], (Leblanc et al., 2008)[2], (Shoushtarian and Negahban-Azar, 2020)[3], (Elbana et al., 2019)[4], (IL&FS Ecosmart Limited, 2009)[5], (India Central Pollution Control Board, Ministry of Environment and Forest, 2006)[6], (Gutiérrez, 2008)[7], (Snyman and Herselman, 2006)[8], (Department of Water Affairs, 2013)[9], (Alemu et al., 2016)[10], (Jeong et al., 2016)[11].

Alternatively, the treated BOTE can be used by other neighbouring industries within the eco-industrial park for non-potable purposes such as construction, cooling and smelting. The use of treated BOTE for irrigation purposes must be carefully considered, and the soil and plants being irrigated must be selected based on the less risk for contamination.

*3.2.5. Biofertiliser and compost*

The digestate contained the contained essential macronutrients: nitrogen, phosphorus and potassium (N:P:K=2:1:1 for optimal conditions), calcium, sulphur, magnesium and micronutrients such as boron, manganese, iron, and molybdenum for use as a biofertiliser (Table 4). The recovery of P, Mg and N in the digestate is assumed to have been aided by the precipitation of struvite while other metals most likely precipitated as sulphide and/or hydroxide complexes. These were observed as white flakes that settled to the bottom of the reactors, particularly under optimal conditions. The optimal conditions produced a digestate with 22.9% carbon, 2.94% hydrogen, 2.09% nitrogen and 1.84% sulphur. The metal concentrations of the digestate were within the recommended limits for class A1a sludge suitable for agricultural use in South Africa and other developing countries leading in bovine leather production, except for Cr (Table 4). Chrome is insoluble in water and it generally attaches to the suspended solids and hence its high concentration in the sludge. Nonetheless, the digestate can be further composted with stabilised organic waste that has minimal Cr concentrations. The type of organic substrate/s and mixing ratios can be optimised depending on the type of soil and the cultivated plant/s. Application of such compost will be beneficial for sandy soils that mainly lack the essential elements for plant growth.

*3.2.6. Concrete and ceramic aggregate*

The high concentration of carbon (229–252 g/kg), Si (5.61–2.75 g/kg) and metals (Table 4) indicated that the digestate may be suitable as a concrete and/or ceramic aggregate. Abreu and Toffoli (2009) successfully incorporated tannery sludge in the manufacture of ceramic tiles and reported a gain in aesthetics (brightness, colour, and texture). Furthermore, this has the benefit of reducing the production costs as less cement and energy will be used. The digestate is a good energy source as it contained about 22.9% carbon, and 2.94% hydrogen. Juel et al. (2017) achieved 15–47% energy savings after adding 10–40% tannery sludge in clay bricks while Kavouras et al. (2015) reported the incineration (500 °C) of tannery sludge to recover Cr (III) and conditioned ash suitable for vitrification. However, co/combustion of digestate offsets volatile toxic heavy metals such as Cr (VI) (Abreu and Toffoli, 2009). The total metal emission limits applicable to digestate combustion/co-combustion in South Africa are 0.05 $mg/m^3$ (Cd and Cr), 0.5 $mg/m^3$ (Sb, As, Pb, Cr, Co, Cu, Mn, Ni, V, Be, Ba, Ag, Sn), 1 $mg/m^3$ (HF), 10 $mg/m^3$ (HCl and TOC), 50 $mg/m^3$ ($SO_2$), and 200–800 $mg/m^3$ ($NO_x$) (Herselman et al., 2009).

*3.3. Process efficiency and inhibition*

A review of previous studies on the AD of TE by (Mpofu et al., 2021a) has reported that $NH_3$ resulting from protein hydrolysis, metals, VOAs, $SO_4^{2-}$ and/or $H_2S$ from sulfidogenesis are the main inhibitors of methanogenesis. Methanogens dictate the minimum solids or hydraulic retention time (S/HRT) as they are the slowest-growing and the most sensitive functional microbes in the consortium.

The control reactors (R18, R19, R20 and R21) and reactors (R5, R16 and R17) treating 100% TY at different ISR generated negligible biogas that was less than the control, regardless of the operating ISR. All the permanently inhibited reactors, including the acetate control reactor (R19) were seemingly active proving that it was only methanogenesis that was inhibited. The reversible inhibited reactors (R2, R11, R14 and R15) operating at 25 or 100%BH suffered short lag phases of 4–6 days (Fig. 2A–D) and were in agreement with the typical regeneration time (5–16 days) for methanogens (Zupančič et al., 2012). All the active reactors produced > 85% of their ultimate $CH_4$ yield within 20 days HRT except for R6 that only produced 40% and required 34 days to achieve this (Fig. 2B).

*3.3.1. Ammonia, volatile organic acids inhibition and pH changes*

The lack of $CH_4$ generation in some of the reactors reflected poor or absent methanogenic activity, but not necessarily a lack of other metabolic processes. The primary mechanism for $NH_3$ release and accumulation (2.3–40.4% after 40 days), was through protein hydrolysis as evidenced by the decrease in protein concentration (1.4–46.2% after 40 days, data not shown). The increase of hydrolysis metabolites concentrations, namely $NH_3$ and VOAs, in some reactors was assumed to be due to an imbalance of AD processes. Achouri et al. (2017) attributed the observed inhibition between day 4 and 12 to the fast formation of VOAs, particularly considering the low operating ISR (=1.5). There was an overall decrease of 11–97% in VOAs initial concentrations (149–1283 mg $CH_3COOH$/L) except for R6 (50% BH, ISR = 1) that suffered an 85% increase to 2382 mg $CH_3COOH$/L. This may have been the cause of permanent inhibition of methanogenesis and dominance of sulfidogenesis in R6. In general, SRB are known to be more resilient to inhibition and they have a higher affinity for hydrogen ($H_2$) and $CH_3COOH$ compared to methanogens. However, Berhe and Leta (2018) reported steady state operations at VOAs concentrations as high as 8300 mg $CH_3COOH$/L.

The $NH_3$ concentration at day 0 (228–484 mg/L) and day 40 (264–620) in all reactors fell within the inhibitory concentration range of 53–1450 mg/L reported by previous studies (Mpofu et al., 2021a). The accumulation of $NH_3/NH_4^+$ led to pH increases above the optimal range of 6.5–7.8 for methanogens in some reactors. This $NH_3/NH_4^+$ buffering capacity most likely played a huge role in restricting pH changes to minimal and in maintaining reactor pH within the optimal range for some reactors. Apart from R6 (50% and ISR=1), the VOA:ALK ratios of all the reactors were within optimal range (< 0.3–0.4) for

**Table 5**
Evaluation of average daily costs at full scale application for a medium sized tannery.

| | |
|---|---|
| **Solid waste and wastewater produced** | |
| B/ovine skins/hides processed (35% hides and 65% skins) | 10000 |
| Weight of skin/hides (tonne) | 115 |
| Weight of shavings produced (tonne) | 11 |
| Weight of chrome splits, trimmings and dust produced (tonne) | 24 |
| Weight of sludge produced (tonne) | 58 |
| Volume of water used ($m^3$) | 2471 |
| Volume of wastewater discharged ($m^3$) | 2300 |
| Carbon emissions (tonnes of $CO_2$ equivalent) | 49.7 |
| Weight of total solid waste produced (tonne) | 93 |
| Average electricity consumption (MWh) | 44 |
| **Operating costs** | |
| Cost of municipal water (US$) | 4948 |
| Cost of wastewater disposal (US$) | 3230 |
| Cost of electricity (US$) | 5348 |
| Cost of landfill disposal of solid waste produced (excluding transport) (US$) | 1080 |
| **Potential savings** | |
| Biogas generated ($m^3$/tVS) | 639 |
| Electric energy production potential (MWh) | 9.89 |
| Reduction in wastewater disposal | 22% |
| Reduction in landfill solid waste disposal | 62% |
| Reduction in electric consumption (%) | 22.5% |
| Reduction in carbon emissions (%) | 38% |
| Potential electricity cost savings (US$) | 1177 |
| Wastewater discharge potential savings (US$) | 711 |
| Reduction in waste disposal costs (US$) | 665 |
| **Potential revenue** | |
| Potential impure sulphur sales (US$) | 1064 |
| Potential biofertiliser/compost sales (US$) | 2752 |

stable reactors (Gao et al., 2015). The alkalinity ($CaCO_3$) in all the reactors increased and suggested microbial utilisation of produced $H^+$ by oxidising homoacetogens, chemolithotrophic sulphur oxidising bacteria (SOB) and/or hydrogenotrophic methanogens (HMs). The alkalinity concentrations (1550–4030 mg$CaCO_3$/L) were within the optimal range (1000–5000 mg$CaCO_3$/L) for steady AD system (Berhe and Leta, 2018).

### 3.3.2. Sulphate and sulphide inhibition

Sulfidogenesis occurred in all the reactors and led to reductions in $SO_4^{2-}$, with concomitant increases in $HS^-$ concentrations over the 40 days S/HRT (Table 2). The majority of the initial reactor COD: $SO_4^{2-}$(1.1–6.3) suggested the likelihood of competition between sulfidogenesis and methanogenesis. The theoretical optimum COD: $SO_4^{2-}$ ratio for significant COD removal by SRB was reported as > 0.67. However, pro-methanogenic COD: $SO_4^{2-}$ ratios as low as 0.5 have been reported under different operating conditions (Omil et al., 1996). The overall decrease in VOAs (11–97%) and $SO_4^{2-}$ (34–85%) from initial concentration range of 300–3800 to 75–2180 mg/L in all reactors (data not shown) proved that both acidogenesis and acetogenesis occurred during the lag phase, and in permanently inhibited reactors. This proved that SRB did not only dominate $H_2S$ generation ($SO_4^{2-}$ reduction), but also utilised hydrolysis metabolites and VOAs in reactors operating at high $SO_4^{2-}$ concentrations (820 mg/L≤$SO_4^{2-}$≤1390 mg/L), particularly R5, R6, R16 and R17 operating at 0% BH (100%TY) and 50%BH at ISR=1. The syntrophic degradation of VOAs by SRB played a major role in improving $B_o$ even without $CH_4$ generation.

The $H_2S$ was mostly solubilised to $HS^-$ at pH > 7 and some of it theoretically precipitated with metals. Precipitation of $HS^-$ with metals can reduce direct $HS^-$ toxicity on functional microbial species, but it can also reduce the bioavailability of essential methanogenic micronutrients. Achouri et al. (2017) and Berhe and Leta (2018) experienced steady state conditions using substrates with high initial total sulphide concentrations of 320 and 132 mg/L at initial pH 7 and pH 6.2 (approximately 180 and 109 mg $H_2S$ /L), respectively. The $H_2S$ concentrations for R1, R2, R4 and R6 (operating at 25–50%BH and ISR = 1–2.5) at day 40 fell close/within the methanogenesis inhibitory range ($IC_{50}$ = 43–125 mg/L at pH 7–8) for suspended sludge (O'Flaherty et al., 1998).

### 3.3.3. Metal inhibition and stimulation

The concentrations of metals were measured in the soluble (filtered) fraction of the reactor contents, which was assumed to represent the bioavailable fraction. The bioavailability of essential metals (Cu, Ni and Zn) collectively reduced in R1, R2 (except Ni), R3, R4, R6 and R8 (except Cu), R14, R15, and R17 (except Ni) while they increased in R5 and R10. Similarly, Ca, Mn, Cr (except R5), Fe (except R5, R11 and R16), K and Na (except R1, R4, R7, R10, R13) and Mg (except R1, R3, R4, R5, R7, R10 and R13) reduced in all the reactors and may have prevented $HS^-$ and metal inhibition. However, the decrease in the bioavailability of essential metals through precipitation and increase of other metals (bracketed) may have contributed to inhibition. It is conceivable that precipitates may have reversibly inhibited functional microorganisms by blocking their access to substrates (Utgikar et al., 2002). Notably, most metals increased in the permanently inhibited reactors (R5, R16 and 17) that mono digested TY.

Additional experiments conducted by the authors at pilot scale with mechanical mixing over a period of 6 months have demonstrated the selection of specific methanogenic archaea *(Methanobacterium, Methanosaeta and Methanosarcina)* and specific genera of SRB *(Desulfovibrio, Desulfomicrobium and Desulfobacterium)* (Kibangou et al., 2021).

### 3.4. Circular bioeconomy in tanneries

The application of optimum conditions at full scale would produce about 20.8 mL (mega liters) of biogas with 12.3 mL recoverable as $CH_4$, when treating 2300 $m^3$ of BH. Alternatively, this can be used to produce approximately 9.89 MWh of electricity that can be used to process 2300–5205 bovine hides, while reducing electricity demand by 22.5% (Table 5). This is based on the assumption that biogas has an average calorific value of 6 kWh/$m^3$ and its conversion efficiency to electricity is 35% (Agustini et al., 2019), while processing a bovine hide requires about 1.9–4.4 kWh (Swartz et al., 2017). The disposal of wastewater in the municipal sewer and landfill disposal of solid waste will be reduced by 22% and 62% while potentially saving US$ 711 and US$ 665, respectively (Table 5). There is a potential revenue of US$ 3816 from the sale of recycled sulphur and biofertiliser/compost for agricultural applications. Additionally, replacing the activated sludge process with AD would reduce carbon equivalent emissions by 38% (19 $tCO_2eq$) based on the assumption that BOTE treatment using the activated sludge process produces 3.15 $tCO_2eq/tCOD_{removed}$ and that producing a MWh of electricity releases 0.90 $tCO_2eq$ (Climate Transparency, 2021; Giaccherini et al., 2017).

This study demonstrated that the full scale application of AD in tannery WWTPs of developing countries presents an opportunity for transitioning to a circular bioeconomy through the establishment of onsite biorefineries for the recovery of resources (biofuels, bioenergy, biofertiliser, sulphur and irrigation water), reduction of carbon emissions, and prevention of waste disposal. This will aid in the sustainable socio-economic development of developing countries whose economies are mainly dependent on fossil based energy and raw materials. However, each tannery must conduct a detailed technoeconomic assessment and market research in order to determine the market potential of the most economically viable recoverable resources and viability of implementing AD (Mpofu et al., 2021a). There is also a need for the upskilling of wastewater treatment practitioners as AD is a complex process that is prone to inhibition particularly when treating TEs. Governments of developing countries must assist tanneries with capital funding and introduce progressive policies, regulations, incentives and subsidies to support the adoption of AD. Furthermore, governments and the private sector can sign long term off take agreements with tanneries for the reuse and recycling of products, particularly sulphur and/or biofertiliser.

## 4. Conclusion

Beamhouse effluent exhibited the most favourable characteristics for anaerobic digestion, and process efficiency and kinetics improved with beamhouse composition and inoculum to substrate ratio up to 100% and 3, respectively. All methanogenic inhibited reactors were active due to the activity of sulphur reducing bacteria. The logistic, modified Gompertz and cone model showed a better fit to the experimental cumulative $CH_4$ data ($0.827 \leq$ Adj $R^2 \leq 0.999$), respectively. The optimum operating conditions at 100%BH, ISR = 2.5 and 20 days retention time were ideal for recovering 377 mL $CH_4$/gVS, 13% and 18% of the inlet sulphur and nitrogen, respectively. Additionally, the process recovered reusable water for irrigation and/or for recycling into the tanning process, and digestate as a biofertiliser and/or ceramic aggregate with energy recovery. The study demonstrated the feasibility of a circular bioeconomy and net positive tannery operations with potential cost savings in electricity demand (22.5%), wastewater disposal (22%) and landfilling of solid waste (62%).

## Declaration of Competing Interest

The authors declare that they have no known competing financial interests or personal relationships that could have appeared to influence the work reported in this paper.

## Acknowledgements

The authors would like to thank the Water Research Commission (WRC) of South Africa for funding this project (K5/2841/3). Any opinion, findings and conclusions or recommendations expressed in this paper are those of the authors and not of the WRC.

## Appendix A. Supporting information

Supplementary data associated with this article can be found in the online version at doi:10.1016/j.psep.2021.12.027.

## References

Abreu, M.A., Toffoli, S.M., 2009. Characterization of a chromium-rich tannery waste and its potential use in ceramics. Ceram. Int. 35, 2225–2234. https://doi.org/10.1016/j.ceramint.2008.12.011

Achouri, O., Panico, A., Ph, D., Derbal, K., Ph, D., Pirozzi, F., 2017. Effect of chemical coagulation pretreatment on anaerobic digestion of tannery wastewater. J. Environ. Eng. 1–5. https://doi.org/10.1061/(ASCE)EE.1943-7870.0001235

Agustini, C.B., da Costa, M., Gutterres, M., 2019. Tannery wastewater as nutrient supply in production of biogas from solid tannery wastes mixed through anaerobic co-digestion. Process Saf. Environ. Prot. 135, 38–45. https://doi.org/10.1016/j.psep.2019.11.037

Alemu, T., Lemma, E., Mekonnen, A., Leta, S., 2016. Performance of Pilot Scale Anaerobic-SBR System integrated with constructed wetlands for the treatment of tannery wastewater. Environ. Process. 3, 815–827. https://doi.org/10.1007/s40710-016-0171-1

Berhe, S., Leta, S., 2018. Anaerobic co-digestion of tannery waste water and tannery solid waste using two-stage anaerobic sequencing batch reactor: focus on performances of methanogenic step. J. Mater. Cycles Waste Manag. 20, 1468–1482. https://doi.org/10.1007/s10163-018-0706-9

Buljan, J., Král, I., 2019. The framework for sustainable leather manufacture (No. 2). Vienna.

Buljan, J., Král, I., 2015. The framework for sustainable leather manufacture. Vienna.

Chou, H.H., Huang, J.S., Chen, W.G., Ohara, R., 2008. Competitive reaction kinetics of sulfate-reducing bacteria and methanogenic bacteria in anaerobic filters. Bioresour. Technol. 99, 8061–8067. https://doi.org/10.1016/j.biortech.2008.03.044

Climate Transparency, 2021. South Africa climate transparency report: comparing G20 climate action towards net zero.

De Morais Ferreira, D., Navoni, J.A., Araújo, A.L.C., Tinoco, J.D., Amaral, V.S., Do, 2019. Wastewater use in agriculture: analytical limits of sewage for impact control in Brazil. Rev. Caatinga 32, 1048–1059. https://doi.org/10.1590/1983-21252019v32n421rc

Department of Water Affairs, 2013. Revision of General Authorisations in terms section 39 of the National Water Act, 1998 (Act number 36 of 1998). South Africa.

Elbana, T.A., Bakr, N., Elbana, M., 2019. Reuse of Treated Wastewater in Egypt: Challenges and Opportunities. Handb. Environ. Chem. 75. pp. 429–453. https://doi.org/10.1007/698_2017_46

Gao, S., Zhao, M., Chen, Y., Yu, M., Ruan, W., 2015. Tolerance response to in situ ammonia stress in a pilot-scale anaerobic digestion reactor for alleviating ammonia inhibition. Bioresour. Technol. 198, 372–379. https://doi.org/10.1016/j.biortech.2015.09.044

Giaccherini, F., Munz, G., Dockhorn, T., Lubello, C., Rosso, D., 2017. Carbon and energy footprint analysis of tannery wastewater treatment: a global overview. Water Resour. Ind. 17, 43–52. https://doi.org/10.1016/j.wri.2017.03.001

Gutiérrez, C., 2008. Standards and thresholds for waste water discharges in Mexico. In: Standards and Thresholds for Impact Assessment. 3. Springer-Verlag, pp. 113–124. https://doi.org/10.1007/978-3-540-31141-6_9

Herselman, J., Burger, L., Moodley, P., 2009. Guidelines for the Utilisation and Disposal of Wastewater Sludge: Requirements for thermal sludge management practices and for commercial products containing sludge. Pretoria.

Holliger, C., Alves, M., Andrade, D., Angelidaki, I., Astals, S., Baier, U., Bougrier, C., Buffière, P., Carballa, M., De Wilde, V., Ebertseder, F., Fernández, B., Ficara, E., Fotidis, I., Frigon, J.C., De Laclos, H.F., Ghasimi, D.S.M., Hack, G., Hartel, M., Heerenklage, J., Horvath, I.S., Jenicek, P., Koch, K., Krautwald, J., Lizasoain, J., Liu, J., Mosberger, L., Nistor, M., Oechsner, H., Oliveira, J.V., Paterson, M., Pauss, A., Pommier, S., Porqueddu, I., Raposo, F., Ribeiro, T., Pfund, F.R., Strömberg, S., Torrijos, M., Van Eekert, M., Van Lier, J., Wedwitschka, H., Wierinck, I., 2016. Towards a standardization of biomethane potential tests. Water Sci. Technol. 74, 2515–2522. https://doi.org/10.2166/wst.2016.336

IL&FS Ecosmart Limited, 2009. Technical EIA guidance manual for common effluent treatment plants. Hyderabad.

India Central Pollution Control Board, Ministry of Environment and Forest, 2006. Characterization of MSW compost and its Application in Agriculture. Parivesh Bhawan.

Jeong, H., Kim, H., Jang, T., 2016. Irrigation water quality standards for indirect wastewater reuse in agriculture: a contribution toward sustainablewastewater reuse in South korea. Water (Switz. ) 8. https://doi.org/10.3390/w8040169

Juel, M.A.I., Mizan, A., Ahmed, T., 2017. Sustainable use of tannery sludge in brick manufacturing in Bangladesh. Waste Manag. 60, 259–269. https://doi.org/10.1016/j.wasman.2016.12.041

Kavouras, P., Pantazopoulou, E., Varitis, S., Vourlias, G., Chrissafis, K., 2015. Incineration of tannery sludge under oxic and anoxic conditions: study of chromium speciation. J. Hazard. Mater. 283, 672–679. https://doi.org/10.1016/j.jhazmat.2014.09.066

Kibangou, V.A., Lilly, M., Mpofu, A.B., de Jonge, N., Oyekola, O.O., Jean Welz, P., 2021. Sulfate-reducing and methanogenic microbial community responses during anaerobic digestion of tannery effluent. Bioresour. Technol. 69, 126308. https://doi.org/10.1016/j.biortech.2021.126308

Leblanc, R.J., Mattews, P., Richard, R.P., Leblan, R.J., Mattews, P., Richard, R.P., 2008. Global atlas of excreta, wastewater sludge, and biosolids management. In: Proceedings of–IWA Conference–Moving forward Wastewater biosolids sustainability technical managerial and public synergy June. United Nations Human Settlements Programme, Nairobi.

Maqbool, A., Ali, S., Rizwan, M., Ishaque, W., Rasool, N., Rehman, Ur, M.Z., Bashir, A., Abid, M., Wu, L., 2018. Management of tannery wastewater for improving growth attributes and reducing chromium uptake in spinach through citric acid application. Environ. Sci. Pollut. Res. 25, 10848–10856. https://doi.org/10.1007/s11356-018-1352-4

Marais, T.S., Huddy, R.J., Harrison, S.T.L., van Hille, R.P., 2020. Demonstration of simultaneous biological sulphate reduction and partial sulphide oxidation in a hybrid linear flow channel reactor. J. Water Process Eng. 34, 101143. https://doi.org/10.1016/j.jwpe.2020.101143

Mekonnen, A., Leta, S., Njau, K.N., 2016. Anaerobic co-treatment of tannery wastewater and cattle dung for biogas production using a pilot scale anaerobic sequencing batch reactor (ASBR) 7, 633–649.

Moraes, B.S., Souza, T.S.O., Foresti, E., 2012. Effect of sulfide concentration on autotrophic denitrification from nitrate and nitrite in vertical fixed-bed reactors. Process Biochem. 47, 1395–1401. https://doi.org/10.1016/j.procbio.2012.05.008

Mpofu, A.B., Kibangou, V.A., Kaira, W.M., Oyekola, O.O., Welz, P.J., 2021b. Anaerobic co-digestion of tannery and slaughterhouse wastewater for solids reduction and resource recovery: effect of sulfate concentration and inoculum to substrate ratio. Energies 14, 2491. https://doi.org/10.3390/en14092491

Mpofu, A.B., Oyekola, O.O., Welz, P.J., 2021a. Anaerobic treatment of tannery wastewater in the context of a circular bioeconomy for developing countries. J. Clean. Prod. 296, 126490. https://doi.org/10.1016/j.jclepro.2021.126490

Mpofu, A.B., Oyekola, O.O., Welz, P.J., 2020. Co-digestion of tannery waste activated sludge with slaughterhouse sludge to improve organic biodegradability and biomethane generation. Process Saf. Environ. Prot. 131, 235–245. https://doi.org/10.1016/j.psep.2019.09.018

O'Flaherty, V., Lens, P., Leahy, B., Colleran, E., 1998. Long-term competition between sulphate-reducing and methane-producing bacteria during full-scale anaerobic treatment of citric acid production wastewater. Water Res. 32, 815–825. https://doi.org/10.1016/S0043-1354(97)00270-4

Omil, F., Lens, P., Hulshoff, L., Lettinga, G., 1996. Effect of upward velocity and sulphide concentration on volatile fatty acid degradation in a sulphidogenic granular sludge reactor. Process Biochem. 31, 699–710.

Sabumon, P.C., 2008a. Development of the Sulphidogenesis Cum Ammonia Removal Process for treatment of tannery effluent. Water Sci. Technol. 58, 391–397. https://doi.org/10.2166/wst.2008.369

Sabumon, P.C., 2008b. Development of a novel process for anoxic ammonia removal with sulphidogenesis. Process Biochem. 43, 984–991. https://doi.org/10.1016/j.procbio.2008.05.004

Saxena, S., Saharan, V.K., George, S., 2019. Modeling & simulation studies on batch anaerobic digestion of hydrodynamically cavitated tannery waste effluent for higher biogas yield COD TS. Ultrason. – Sonochem. 58, 104692. https://doi.org/10.1016/j.ultsonch.2019.104692

Shoushtarian, F., Negahban-Azar, M., 2020. World wide regulations and guidelines for agriculturalwater reuse: a critical review. Water (Switzerland) 12. doi: 10.3390/W12040971.

Snyman, H., Herselman, J., 2006. Guidelines for the Utilisation and Disposal of Wastewater Sludge: Requirements for the agricultural use of sludge. Pretoria.

Swartz, C.D., Jackson-Moss, C., Rowswell, R., Mpofu, A.B., Welz, P.J., 2017. Water and Wastewater Management in the Tanning and Leather Finishing Industry. Water Research Commission, Pretoria.

Thanh, P.M., Ketheesan, B., Yan, Z., Stuckey, D., 2016. Trace metal speciation and bioavailability in anaerobic digestion: a review. Biotechnol. Adv. 34, 122–136. https://doi.org/10.1016/j.biotechadv.2015.12.006

Utgikar, V.P., Harmon, S.M., Chaudhary, N., Tabak, H.H., Govind, R., Haines, J.R., 2002. Inhibition of sulfate-reducing bacteria by metal sulfide formation in bioremediation of acid mine drainage. Environ. Toxicol. 17, 40–48. https://doi.org/10.1002/tox.10031

Vazifehkhoran, A.H., Shin, S.G., Triolo, J.M., 2018. Use of tannery wastewater as an alternative substrate and a pre-treatment medium for biogas production. Bioresour. Technol. 258, 64–69. https://doi.org/10.1016/j.biortech.2018.02.116

Zupančič, G.D., Viktor, G., Grilc, V., 2012. In: Kumar, Sunil, Bharti, A. (Eds.), Anaerobic Treatment and Biogas Production from Organic Waste. Management of Organic Waste, Slovenia, pp. 1–27. https://doi.org/10.5772/1382